Inorganic Chemistry

Article

pubs.acs.org/IC

Synthesis and Oxidative Reactivity of 2,2′-Pyridylpyrrolide Complexes of Ni(II)

Nikolay P. Tsvetkov, Chun-Hsing Chen, José G. Andino, Richard L. Lord,† Maren Pink, René W. Buell, and Kenneth G. Caulton*

Department of Chemistry, Indiana University, 800 E. Kirkwood Avenue, Bloomington, Indiana 47405-7102, United States

Supporting Information

ABSTRACT: Synthesis and characterization of divalent nickel complexed by 2-pyridylpyrrolide bidentate ligands are reported, as possible precursors to complexes with redox active ligands. Varied substituents on the pyrrolide, two CF_3 (L^2), two ^{t}Bu (L^0), and one of each type (L^1) are employed and the resulting $Ni(L^n)_2$ complexes show different Lewis acidity toward CO, H_2O, tetrahydrofuran (THF), or MeCN, the L^2 case being the most acidic. Density functional theory calculations show that the frontier orbitals of all three $Ni(L^n)_2$ species are localized at the pyrrolide groups of both ligands and $Ni(L^n)_2^+$ can be detected by mass spectrometry and in cyclic voltammograms (CVs). Following cyclic voltammetry studies, which show electroactivity primarily in the oxidative direction, reactions with pyridine N-oxide or Br_2 are reported. The former yield simple *bis* adducts, $Ni(L^2)_2(pyNO)_2$ and the latter effects electrophilic aromatic substitution of the one pyrrolide ring hydrogen for both chelates, leaving it brominated.

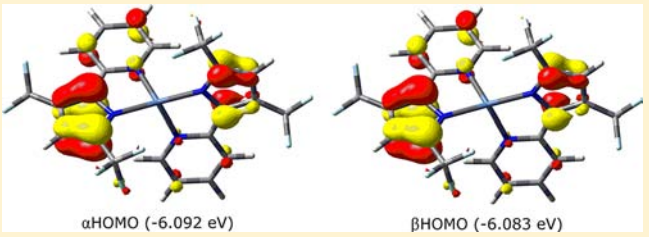

INTRODUCTION

The goal here is a ligand type which combines electron donating amide character with modular steric modification, all for the purpose of developing a new variety of redox active ligand. The pyridyl pyrrolides (Scheme 1; *n* in L^n indicates the number of CF_3 groups) appear to offer this possibility since their synthesis, discovered by the McNeill group,[1] involves a convenient ring closure of a beta diketone with an amino-methylpyridine. Reported here are efforts at inner sphere oxidation of $Ni^{II}(L^n)_2$ complexes of these monoanionic ligands, to oxidatively install one or two new ligands, and with a goal of accessing molecules like $(L^n)_2NiO$, $(L^n)_2Ni(NR)$, or $(L^n)_2NiCl_q$. These ligands have been previously of interest for optoelectronic applications, as well as monoanionic chelate structural elements, but not for redox activity.[2−14] Because of the synthetic method and the ready availability of beta diketones, including those with two different substituents, a wide range of pyridylpyrroles become available, to allow testing, in metal complexes, of the influence on reactivity of electron donating and withdrawing groups, and also of differing steric effects. Although related NN′ ligands, including[15−19] imino-pyrrolides, have been studied (**1**−**3** in Scheme 1), this was mainly for olefin polymerization purposes, and was structurally based,[20−22] without serious consideration of ligand-based redox activity.

Of interest is the degree of π-donation from the pyrrole to a metal, and how this is influenced by the *constraints* of it being in a chelate with a pyridine as the second donor. There is strong evidence that pyrrolides greatly enhance the reducing power of already low valent transition metals.[23−29] For comparison, physical organic studies of pyrroles have shown that they are π-donors when attached via N or via any pyrrole ring carbon.[30,31] As a substituent on an aryl (pyridine) ring, a pyrrolide thus gives amide character to the pyridine partner, as illustrated in **4**, provided there is conjugation between the two rings. It is relevant to note that, in comparison to the gas phase ionization potential of benzene, 9.25 eV, the values for pyridine (9.27 eV) and pyrrole (8.2 eV)[9−14] show the donor power/ease of oxidation of pyrrole itself.

Reported here is an initial survey of the steric and electronic properties of this ligand class attached to nickel(II), to test the extent to which pyrrole ring substituents can modulate donor power, and perhaps also the ability of the ligand to be oxidized. On pyrrole itself, these substituents cause[32] a highest occupied molecular orbital (HOMO) energy *variation* of over 1.7 eV. Alternatively the adiabatic first ionization potential of HL^n varies from 8.25 eV (n = 2) to 6.86 eV (n = 0).[32] Finally it is of interest to evaluate whether an *ortho* CF_3 substituent on the pyrrole can resist attack by a highly electrophilic metal center so that the electrophilicity can persist and be focused on bimolecular reactivity. For comparison, it is known that a ^{t}Bu substituent adjacent to pyrrole nitrogen can be attacked by a metal center in a pyridylpyrrolide.[2] Note also (Scheme 2) that the properties conferred on a metal by L^n are very different from the seemingly analogous (i.e., same donor functionalities) beta-diketiminate and dipyrromethene ligands.[33,34]

It is worth noting that pyridylpyrrolides differ from the many redox active ligands that are currently being studied[35−50] since those are generally 2-fold symmetric, with two identical donors

Received: May 10, 2013
Published: August 2, 2013

   dx.doi.org/10.1021/ic4011746 | *Inorg. Chem.* 2013, 52, 9511−9521

Scheme 1

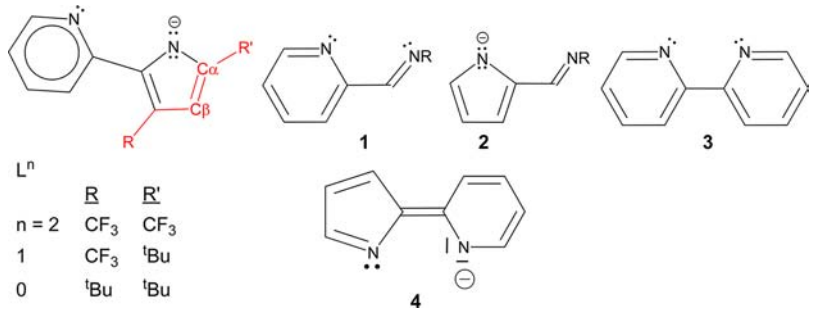

Scheme 2

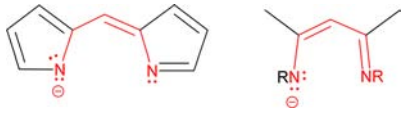

(monoiminoquinones, while not C_2 symmetric, nevertheless involve analogous donors). Pyridylpyrrolides attached to a redox active metal offer pyridine π^* orbitals as an electron acceptor, and pyrrolide occupied π orbitals as a donor, when a pyridylpyrrolide/metal complex is reduced or oxidized, respectively. They thus represent a push/pull pair, not only to each other, but also toward the redox chemistry of an attached metal. This will modulate the redox potential of the combined metal chelate system. In addition, this lack of symmetry in the bidentate ligand makes $M(L^n)_2$ *complexes* of less than D_{2d} symmetry (maximally C_2 symmetric), a factor explored here.

The advantage of installing two pyridylpyrrolides on a single metal is to explore the degree to which such a ligand pair can be *collectively* redox active, hence subject to either electron loss or gain, when the overall metal complex undergoes redox change. If the ligand type is indeed redox active, then this becomes a vehicle for storing redox equivalents at the ligand which exceed the maximum redox capacity of the metal itself. While pyrroles themselves are well-known for being oxidizable, the rapid (but undesirable here) follow-up coupling of the radical cations to form oligo- and polypyrroles[51−54] will perhaps be less likely if the radical cation is bound to a metal center. Throughout all this work, the fact that the pyrrole nitrogen π lone pair is to some extent "committed" to the aromaticity of pyrrole is modulated by the fact that the resonance energy of pyrrole is less than that of benzene by 10−15 kcal/mol.[55]

Our goal of inner sphere oxidation of $Ni(L^n)_2$ complexes, to oxidatively install one or two new ligands, also hinges on steric accessibility to the metal, in molecules like $(L^n)_2NiO$, $(L^n)_2Ni(NR)$, or $(L^n)_2NiCl_q$. Are such $Ni(L^n)_2$ complexes sterically saturated, or is there room for them to bind additional ligands, as is essential to install halo, oxo, or imide ligands by atom transfer? We describe here evidence for binding of reagents to the more electrophilic L^2 complexes of nickel.

RESULTS

Synthesis and Characterization of Nickel Pyridylpyrrolides. In a redox approach to $Ni(L^n)_2$ complexes, Ni powder does not react with HL^2 in tetrahydrofuran (THF) at 25 °C during 12 h. Reaction of $NiCl_2(THF)_x$ with KL^n is more successful, giving a single product for each L^n, but at a rate which decreases with increasing CF_3 content. The products are paramagnetic, hence not planar nickel, and contain symmetry equivalent L^n ligands; for comparison, a platinum analogue[4] is planar, but step-distorted, apparently because of steric conflict between the two chelates. The L^1 example for nickel shows one ^1H NMR ^{t}Bu signal (^{t}Bu at C5) and five signals for ring hydrogens, while the L^0 example shows two ^{t}Bu signals, only one of which has a similar chemical shift to the L^1 case, with the other ^{t}Bu (at C3) not shifted much from the diamagnetic region (at ∼2 ppm, and sharper). This means that the ^{t}Bu more distant from the pyrrole nitrogen (i.e., the new one present in L^0 but absent in L^1) suffers less influence of the paramagnetic metal. Proton NMR is thus very useful, with even very large chemical shifts observed (>200 ppm). The ^{19}F NMR of $Ni(L^1)_2$ shows a signal shifted about 43 ppm from the value in HL^1, but the resonance is sharp and thus very useful for analytical purposes; $Ni(L^2)_2$ shows two ^{19}F NMR signals. Evans' method of magnetic susceptibility measurements[56] show that these complexes have two unpaired electrons per nickel; the μ_{obs} value for $Ni(L^0)_2$ is 2.45 μ_B which is only slightly lower than the expected value of 2.83 μ_B. The atmospheric pressure chemical ionization (AP CI) positive ion mass spectrum of $Ni(L^1)_2$ and of $Ni(L^0)_2$ each show a signal for both M^+ (intact molecular ion) and MH^+; both of these neutral complexes can thus be oxidized, in a mass spectrometer, by one electron, consistent with some redox active behavior at the ligand. The most electron poor ligand, $Ni(L^2)_2$ shows an M^- monoanion in its *negative* ion AP CI mass spectrum, consistent with some combination of reduction of nickel and/or the chelate; conversely, no positive ion M^+ is seen. Most surprising is that the obtained product, from THF solvent, for L^1 is red while that for L^2 is pale yellow-green, both observed in THF or toluene solution and in the solid state; both are still paramagnetic, however. Different colors might suggest dramatic substituent-dependent structural differences. However, in fact, this difference is due to adduct formation.

Single crystal structure determination of this yellow-green $Ni(L^2)_2$ product, recrystallized from pentane, revealed (Figure 1) that a THF molecule from the synthetic solvent remains attached to nickel, to give a five-coordinate structure; this THF is apparently lost under the mass spectrometric sampling conditions. The structure is idealized C_2 symmetric, closer to trigonal bipyramidal, with pyrrolide ligands axial (angle 179.40(5)°) and the two pyridyl ligands compressed to a (very small) interligand angle of 101.68(5)°. Because the py-Ni-py angle is considerably less than the 120° of a perfect trigonal bipyramid, the structure might also be called "saw horse," or "see-saw", as found in the SF_4 structure. The Ni/N distances to pyridine are only about 0.02 Å longer than to pyrrolide. Each chelate is essentially planar, and THF oxygen is coplanar with its three substituents. Misalignment of the

dx.doi.org/10.1021/ic4011746 | Inorg. Chem. 2013, 52, 9511−9521

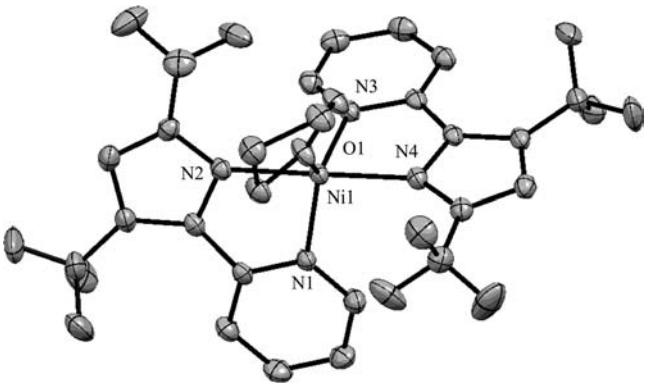

Figure 1. ORTEP view (50% probabilities) of the nonhydrogen atoms of $Ni(L^2)_2(THF)$. Unlabeled atoms are carbons, or the fluorines on CF_3 groups. Selected structural parameters: Ni1–N2, 2.0082(13) Å; Ni1–N4, 2.0156(13); Ni1–N3, 2.0283(13); Ni1–N1, 2.0324(13); Ni1–O1, 2.1278(11); N2–Ni1–N4, 179.40(5)°; N2–Ni1–N3, 99.33(5); N4–Ni1–N3, 80.63(5); N2–Ni1–N1, 80.75(5); N4–Ni1–N1, 99.85(5); N3–Ni1–N1, 101.68(5); N2–Ni1–O1, 89.46(5); N4–Ni1–O1, 90.09(5); N3–Ni1–O1, 127.64(5); N1–Ni1–O1, 130.67(5); C26–O1–C23, 109.84(12); C26–O1–Ni1, 126.93(9); C23–O1–Ni1, 123.21(9).

pyridine lone pairs is only modest (angle C(para)–N–Ni > 174.6°). The NMR spectrum of $Ni(L^2)_2(THF)$ dissolved in benzene shows 5 paramagnetically shifted peaks for aromatic ring hydrogens, and two of double intensity (due to coordinated THF), also shifted. Proton NMR spectra of the THF adduct illustrate that the paramagnetism shifts aryl protons much more dramatically than those of THF, consistent with spin density communication primarily through the π system; the singly occupied molecular orbitals (SOMOs) thus have demonstrable L^2 ligand character.

Four Coordinate $Ni(L^2)_2$ and Its Lewis Acidity. While the yellow-green THF adduct of $Ni(L^2)_2$ crystallizes from pentane solution at −40 °C, THF binding is weak enough that slow removal of volatiles from a pentane or benzene solution of $Ni(L^2)_2(THF)$ furnishes a red solid which is four coordinate $Ni(L^2)_2$. The color change for $Ni(L^2)_2$ is thus due to adduct formation, with the THF-free material being red. Vacuum sublimation is an especially effective way to remove coordinated THF from $Ni(L^2)_2(THF)$, as well as heating in vacuum, followed by extraction of the resultant $Ni(L^2)_2$ into benzene. Conversely, addition of 3 equiv of THF to $Ni(L^2)_2$ in benzene or dichloromethane gives an immediate color change to green with essentially complete conversion (confirmed by NMR spectroscopy) to the adduct $Ni(L^2)_2(THF)$. The ^{19}F and ^1H NMR spectra of $Ni(L^2)_2$ and its THF adduct are quite different, enabling them to be distinguished easily by NMR. However, the ^1H and ^{19}F NMR at 25 °C of a solution containing a mixture of $Ni(L^2)_2$ and $Ni(L^2)_2(THF)$ shows only concentration-weighted averaged signals characteristic of fast exchange of THF between the two.

Crystals grown by cooling a concentrated solution of THF-free $Ni(L^2)_2$ in pentane showed further support for the high Lewis acidity of this molecule: the unit cell is an ordered 1:1 mixture of $Ni(L^2)_2$ and $Ni(L^2)_2(H_2O)$. The composition of these crystals (Figure 2) enables a good comparison of structural change which accompanies adduct formation by the Lewis acidic $Ni(L^2)_2$. Comparison reveals that increasing coordination number by one water molecule lengthens Ni–N(pyrr) distances by 0.06 Å, but Ni–N(py) distances by only 0.03 Å. While the N–Ni–N angle between two pyrrolides in $Ni(L^2)_2$ is already large, at 157.76(14)°, it increases to 178.76(14)° in the water adduct, since these pyrrolide nitrogens are axial in the ∼trigonal bipyramidal structure, as they are in the THF adduct also. The angle between pyridyl nitrogens in $Ni(L^2)_2$ is 104.33(13)°, and decreases to 97.57(13)° in the water adduct. This shows that $Ni(L^2)_2$ clearly has the ability to bind a fifth ligand, which is a positive sign for potential inner sphere redox reactivity. In general, the water adduct is structurally similar to the THF adduct, and both are paramagnetic. The angle between the two NiNN planes (both N in a given chelate) is 84.9° for the four coordinate species, and 88.9° for the five coordinate species. This shows that two planar L^2 ligands can achieve near-orthogonality even when the N(pyrr)–Ni–N(pyrr) angle is far larger than the tetrahedral angle. Finally the water adduct shows short intramolecular contacts between the water oxygen and the two fluorines on two different CF_3 groups (2.88 and 2.98 Å), so this hydrogen bonding confers additional stability to the adduct. This hydrogen bonding is also seen in the geometry

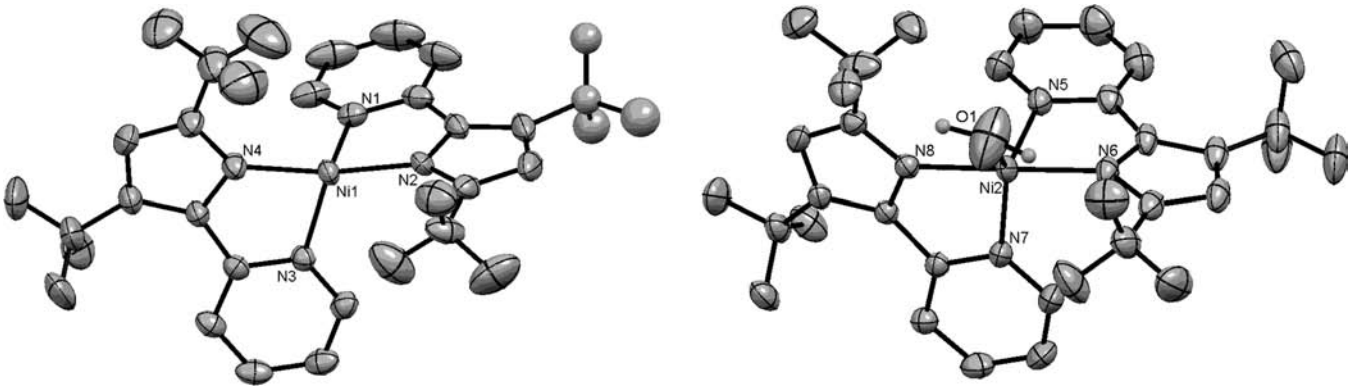

Figure 2. ORTEP view (50% probabilities) of the structure of $Ni(L^2)_2{\cdot}Ni(L^2)_2(H_2O)$ with hydrogens omitted for clarity (water hydrogens are illustrated). Unlabeled atoms are carbons, or fluorine in CF_3 groups. Selected structural parameters: Ni1–N1, 1.994(3) Å; Ni1–N2, 1.935(3); Ni1–N3, 2.002(3); Ni1–N4, 1.932(3); Ni2–O1, 2.206(5); Ni2–N5, 2.035(4); Ni2–N6, 1.993(3); Ni2–N7, 2.030(3); Ni2–N8, 1.980(3); N1–Ni1–N2, 82.66(14); N1–Ni1–N3, 104.33(13); N2–Ni1–N3, 114.74(13); N1–Ni1–N4, 108.25(15); N2–Ni1–N4, 157.76(14); N3–Ni1–N4, 82.02(13); O1–Ni2–N5, 122.7(2); O1–Ni2–N6, 87.84(17); N5–Ni2–N6, 81.06(13); O1–Ni2–N7, 139.7(2); N5–Ni2–N7, 97.57(13); N6–Ni2–N7, 99.47(12); O1–Ni2–N8, 90.94(16); N5–Ni2–N8, 99.36(12); N6–Ni2–N8, 178.74(13); N7–Ni2–N8, 81.67(12).

dx.doi.org/10.1021/ic4011746 | Inorg. Chem. 2013, 52, 9511–9521

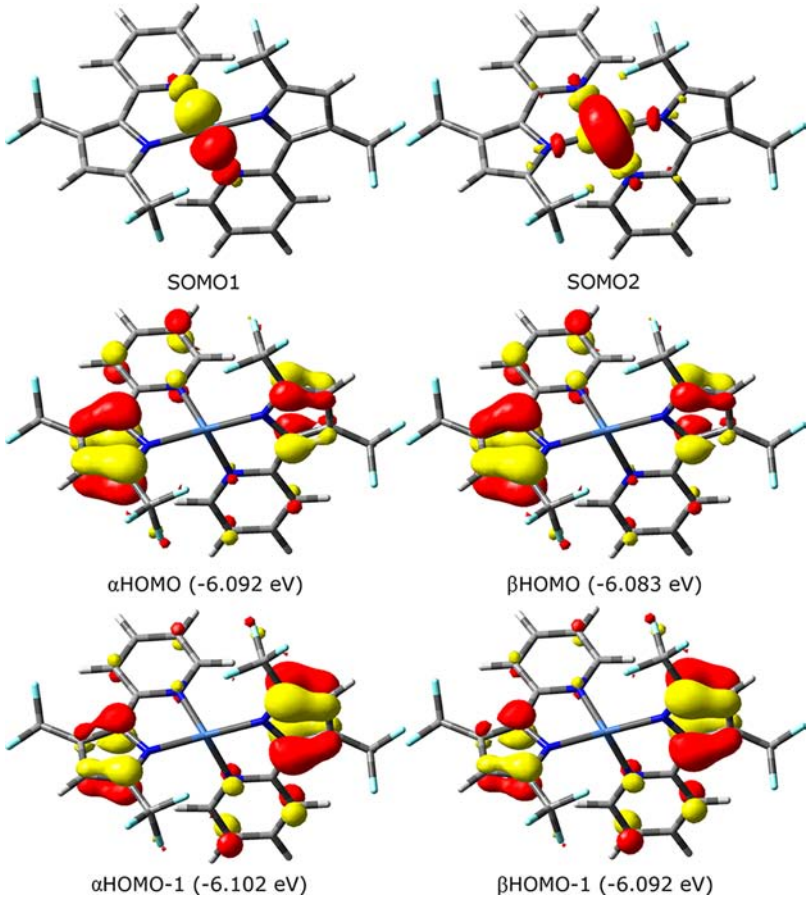

Figure 3. Isodensity plots (0.05 au) of the frontier orbitals of triplet $Ni(L^2)_2$.

resulting from density functional theory (DFT) studies of this adduct.

L^n Substituent Dependence of Reactivity with Water. The above water adduct apparently arises from adventitious water during crystal growth. Addition of stoichiometric water to a benzene solution of $Ni(L^2)_2$ causes an immediate color change to yellow-green, forming a paramagnetic product with NMR spectra distinct from that of four coordinate $Ni(L^2)_2$, demonstrating again the Lewis acidity of the fluorinated ligand case. Delivery of an additional 2 equiv of water to this solution shows only a single resonance for water protons (assignment confirmed by repeating the experiment with D_2O and observing ^2H NMR), indicating rapid exchange of free and coordinated water. In contrast, addition of stoichiometric water to a benzene solution of $Ni(L^0)_2$ shows growth of the NH signal of free HL^0 within 10 min, showing the water sensitivity of this most Brønsted basic of the chelate ligands.

Seeking Other Adducts. Addition of 1 atm CO to a benzene solution of $Ni(L^2)_2(THF)$ gives no change in any resonances, indicating the absence of adduct formation by CO. While $Ni(L^2)_2$ reversibly binds THF but shows no ability to bind CO, $Ni(L^1)_2$ and $Ni(L^0)_2$ show no tendency to bind CO, MeCN, or THF. Thus the heavily fluorinated pyridyl pyrrolide ligand is necessary to elicit spectroscopically detectable Lewis acidity from the NiL_2 complex, and it functions as a hard Lewis acid, not one which can function as a π base. This effect of fluorinated substituents causing increased Lewis acidity has been observed in Pd(II) beta-diketonate coordination chemistry.[57]

Density Functional Theory Study of $Ni(L^n)_2$. *a. Structure.* DFT geometry optimization for triplet $Ni(L^2)_2$ (see Supporting Information) yields a structure that is not regular tetrahedral or trans planar, but an intermediate structure, severely flattened from tetrahedral, with the pyrrolide nitrogens transoid (angle 167°) and the pyridine nitrogens cisoid (angle 108°). The metal nitrogen distances are 2.06 Å to pyridine and 1.96 Å to pyrrolide. The structure has idealized C_2 symmetry, in agreement with the conclusions from NMR spectroscopy. The DFT geometry closely captures the observed (X-ray) features of the structure of $Ni(L^2)_2$, in particular the small angle between the pyridyl nitrogens. A general theoretical treatment of this intermediate four-coordinate structure has been published,[58] and shows the influence of a variety of factors. In our case, an additional feature is steric repulsion between cis donors, which must surely preclude a planar structure. However, is it possible that the nontetrahedral structure is dictated by internal *structural constraints* of the chelate? We believe that this cannot be true, since d^{10} zinc pyridylpyrrolide complexes with H or Me or ^{t}Bu substituents[5,59] are much closer to tetrahedral (ZnN_2/ZnN_2' dihedral angles 80.2, 81.8, and 88.1°), without the distortion found here for nickel; the structure for $Ni(L^2)_2$ is thus dictated by electronic factors of the d^8 configuration. Noteworthy is that this distortion for $Ni(L^2)_2$ is possible without sacrificing the planarity of the two rings in a given chelate: the dihedral NCCN angles within each chelate are less than 3°. Misalignment of the nitrogen lone pairs is limited to the extent that pyridine *para* C−N−Ni angles are all >174°. Pyrrolide nitrogen lone pair misdirection is somewhat greater, due in part to the constraint of the five membered ring

dx.doi.org/10.1021/ic4011746 | *Inorg. Chem.* 2013, 52, 9511−9521

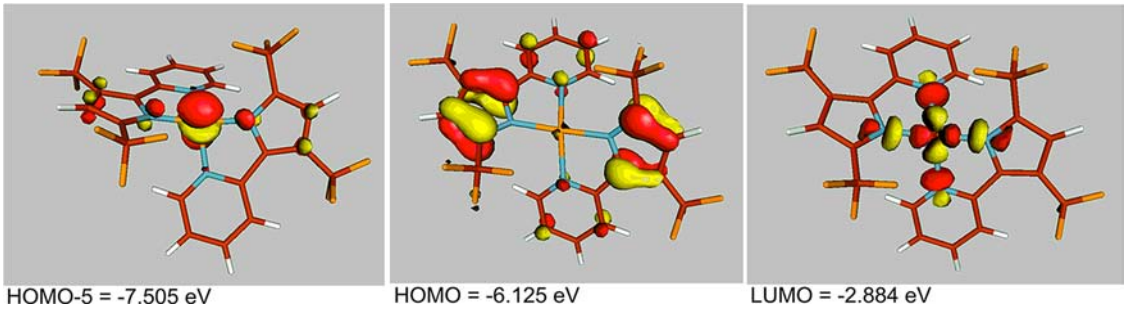

Figure 4. Isodensity plots (0.05 au) of z^2, HOMO, and LUMO of singlet $Ni(L^2)_2$.

involving nickel; the two Ni−N−Cα angles involving pyrrolide are typically unequal, at 115° and 138°, and this feature will be a factor in cases where the pyridyl pyrrolide ligand becomes monodentate.[4]

b. Frontier Orbitals. Shown in Figure 3 are the frontier orbitals of triplet $Ni(L^2)_2$. The highest energy *doubly* occupied orbitals in both the α and β subspaces are nearly degenerate and localized on the pyrrolides, and the SOMO1 and SOMO2, which illustrate the character of the *singly* occupied orbitals, are metal-based (a linear combination of the z^2 and $x^2 - y^2$ orbitals) in agreement with our expectation of a high-spin Ni^{II} center. It was difficult to identify the occupied partners of the unoccupied metal-based LUMOs, and therefore a corresponding orbital analysis[60−63] (Supporting Information, Figure SA) was performed to confirm that these (Figure 3) are indeed the SOMOs. This assertion is further supported by visualizing the spin density (Supporting Information, Figure SA); the Mulliken spin population analysis shows 82% of the spin at Ni and 17% at the four ligating nitrogens.

c. A Planar Singlet Alternative? The traditional sorting of four-coordinate nickel(II) complexes has tetrahedra as triplet states ("high spin") and planar structures as singlets ("low spin"). However, the structures of $Ni(L^n)_2$ are neither of these extremes. In the case at hand, this structure/spin state correlation was tested by geometry optimization of a singlet state for $Ni(L^2)_2$. This gives a structure with trans angles of 165° (between pyrrolide N), hence no change from triplet, and 143° (between pyridyl N), hence a dramatic change *toward* planar, but still not truly planar. On going from triplet to singlet, all Ni−N distances shorten by about 0.07 Å, all consistent with emptying antibonding Ni/N interactions in two half-filled orbitals by putting both electrons in the z^2 orbital (Figure 4) of the more planar singlet, with $x^2 - y^2$ thus empty. The triplet is calculated to be 9 kcal/mol more stable than this singlet. A truly planar MN_4 substructure is found for the Pt analogue,[4] where the two chelate planes are "stepped," to minimize interchelate repulsions. The frontier orbitals of singlet $Ni(L^2)_2$ show (Figure 4) that the lowest unoccupied molecular orbital (LUMO), like that of a conventional four-coordinate singlet species, is $x^2 - y^2$, at high energy because it is σ^*_{Ni-N}. The HOMO is pyrrolide localized, looking very much like some of the frontier orbitals (Figure 3) of the triplet $Ni(L^2)_2$. Thus, the most easily removed electron of singlet $Ni(L^2)_2$ is from the pyrrolide groups, not from nickel. The ligand is redox active.

Electrochemical Evaluation of Redox Behavior. Every ligand must withstand attack by its reactive environment. Here this translates into bond cleavage reactivity at the pyrrolide. Upon attempted oxidation of these $Ni(L^n)_2$ compounds, the electrophilic character of high-valent transition metals coordinated to pyrrolide nitrogens, as well as pyrrolide CF_3 substituents, should leave the pyrrolide less vulnerable to carbon/carbon coupling or electrophilic aromatic attack.

Cyclic voltammograms (CVs) ($[(n\text{-}Bu)_4N]PF_6$ supporting electrolyte, 25 mV s^{-1}) were recorded for the two extreme cases, L^0 and L^2, in both oxidative and reductive directions. $Ni(L^0)_2$ is redox inactive, in the range 0 to −2 V, while $Ni(L^2)_2$ shows a weak and irreversible reductive wave below −1.75 V (all referenced to Fc/Fc^+), both recorded in CH_2Cl_2 (see Supporting Information). Also in CH_2Cl_2, an irreversible oxidative wave is seen (Figure 5) for $Ni(L^2)_2$ with an anodic

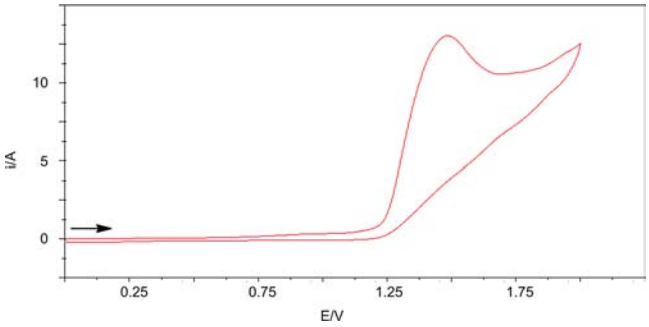

Figure 5. CV of $Ni(L^2)_2$ (using 0.1 M $[(n\text{-}Bu)_4N]PF_6$ in CH_2Cl_2, 25 mV s^{-1}).

peak maximum at +1.5 V. In agreement with the greater donor power of the L^0 chelate, $Ni(L^0)_2$ shows (Figure 6) two oxidative waves in the range 0 to +1.75 V, each of which is quasi reversible at 25 mV s^{-1}; these *two* are clearly not both initiated at divalent nickel, and are more easily understood by the idea of ligand participation in the oxidation.

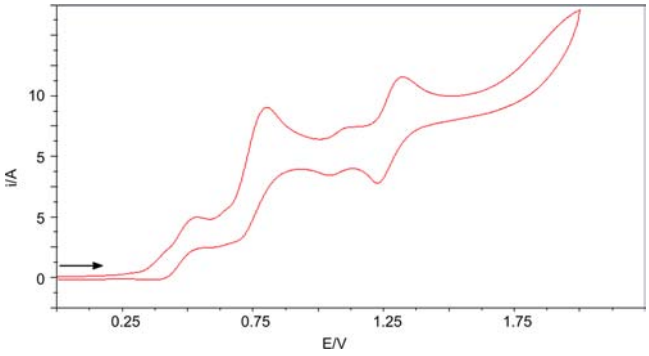

Figure 6. CV of $Ni(L^0)_2$ (using 0.1 M $[(n\text{-}Bu)_4N]PF_6$ in CH_2Cl_2, 25 mV s^{-1}) showing two quasi reversible oxidations with E_{pa} = 0.8 and 1.35 V. Weak current flow at E_{pa} of 0.5 and 1.0 V is due to impurity.

dx.doi.org/10.1021/ic4011746 | Inorg. Chem. 2013, 52, 9511−9521

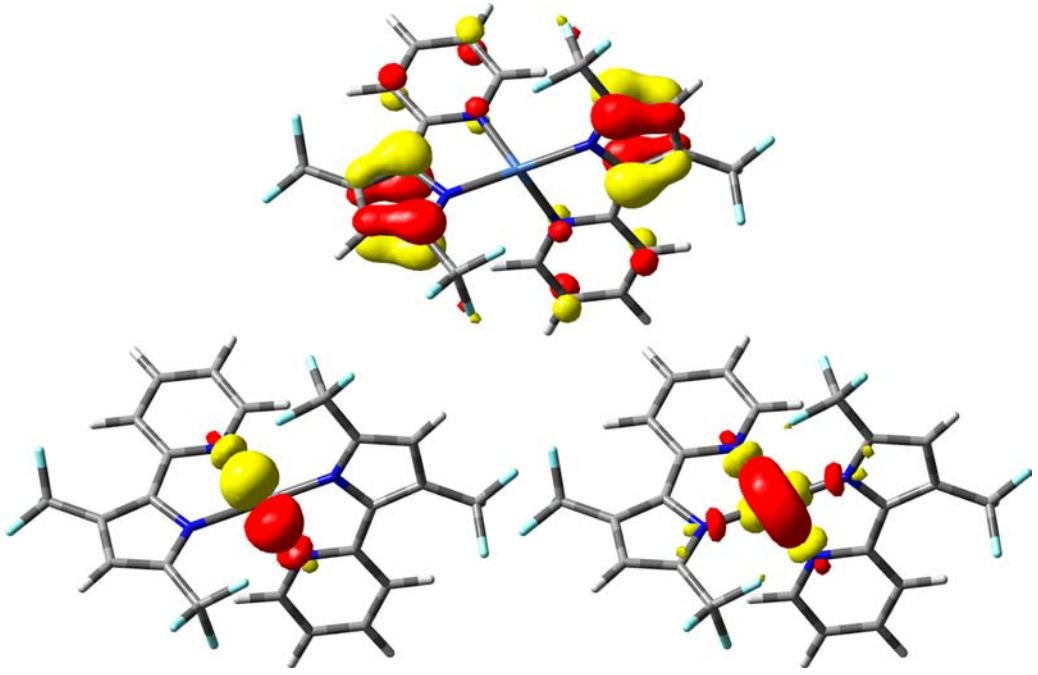

Figure 7. Isodensity plots (0.05 au) of the singly occupied orbitals of $S = 3/2$ $Ni(L^2)_2^+$.

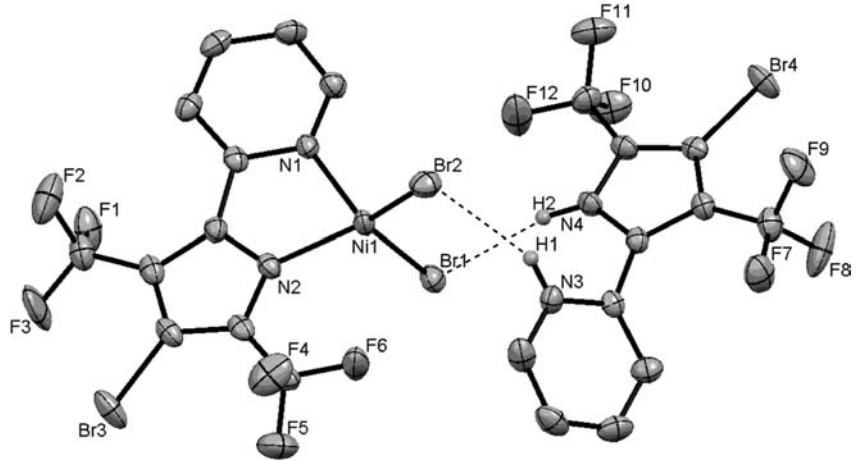

Figure 8. ORTEP view (50% probabilities) of the nonhydrogen atoms of $[H_2{}^{Br}L^2][Ni({}^{Br}L^2)Br_2]$. Unlabeled atoms are carbons (H involved in hydrogen bonding are illustrated). Selected structural parameters: Br1−Ni1, 2.3794(10); Br2−Ni1, 2.3595(10); Ni1−N1, 1.995(5); Ni1−N2, 1.960(4); Br1−Ni1−Br2, 117.41(4); Br1−Ni1−N1, 105.51(14); Br2−Ni1−N1, 114.43(13); Br1−Ni1−N2, 113.38(14); Br2−Ni1−N2, 117.82(15); N1−Ni1−N2, 82.40(19).

DFT Study of the Monocation. What are the geometric and electronic structures (e.g., internal charge distribution) of the $Ni(L^2)_2^+$ cation detected by cyclic voltammetry and mass spectrometry? The geometry optimized structure of quartet $Ni(L^2)_2^+$ is, regarding the NiN_4 substructure, within 0.01 Å and 0.9°, identical to that of its neutral (triplet), and one of the three singly occupied orbitals of the cation has considerable pyrrolide π character (Figure 7). Spin density in this quartet is 55% on nickel and 31% equally on the two pyrrolides and 14% equally on the two pyridyls (Supporting Information, Figure SB).[64]

The largest structural changes (see Supporting Information) upon oxidation are to bond lengths *within* both pyrrolide rings, and these are shorter or longer depending on the bonding/antibonding character of the SOMO: the two Cα/Cβ distances shorten by ∼0.02 Å and the Cβ/Cβ lengthen ∼0.02 Å upon oxidation, completely in agreement with the expectation from one SOMO in Figure 7.[65] The monocation still has the sawhorse geometry (i.e., sterically open), so its unsaturation should easily be satisfied by binding of a Lewis base following oxidation. This can contribute to the irreversible anodic responses observed in the CVs taken in weak donor solvents.

Chemical Oxidation. *Bromine.* Reaction of $Ni(L^2)_2$ with Br_2 (1:1 mol ratio) in CH_2Cl_2 at −40 °C, followed by crystallization by layering with pentane, gave crystalline solid characterized by X-ray diffraction (Figure 8) as $({}^{Br}L^2H_2)[({}^{Br}L^2)NiBr_2]$. Here ${}^{Br}L^2$ signifies that the one ring hydrogen (at C4 or C$_\beta$) of L^2 has been replaced by Br. The reaction of $Ni(L^2)_2$ with Br_2 was studied in CH_2Cl_2 at mole ratios of 1:1 and 1:0.5. In each case the product was the same: $({}^{Br}L^2H_2)[({}^{Br}L^2)NiBr_2]$. Hydrogen bonds are indeed present in the solid, one from each NH proton of the ${}^{Br}L^2H_2$ cation to a different

dx.doi.org/10.1021/ic4011746 | *Inorg. Chem.* 2013, 52, 9511−9521

bromide in the complex anion (Figure 8). Finally the anionic nickel species here is tetrahedral, consistent with spin triplet Ni^{II}. Paramagnetism is indicated by the observed NMR chemical shifts of this salt. This salt product identity yields a full material balance, where the two L^2 ligands of $Ni(L^2)_2$ have undergone electrophilic aromatic CH substitution, with the two protons captured by the nitrogens of one ligand. It also indicates that the reaction has taken place with a $Ni:Br_2$ mole ratio of 1:2 (i.e., distinct from the ratios employed). Seeking a different product by avoiding any excess Br_2 the reaction was therefore repeated with very *slow addition* of the Br_2 solution *to* the nickel complex solution held at −40 °C. This showed no change in the product. The ^1H NMR spectrum of the observed product shows, in the range +250 to −50 ppm, only 3 broad signals, which makes it impossible to confidently assign them. There are no sharp signals which might be attributed to the diamagnetic cation. Curiously, the ^{19}F NMR spectrum shows only one peak, full width at half height of ∼4 ppm, in spite of the expectation that there should be four chemical shifts, two of which are in a diamagnetic species. Apparently hydrogen bonding between cation and anion, enforcing strong ion pairing, can cause paramagnetic effects even in the intrinsically diamagnetic cation. It is significant that both chelates have been brominated, not only one. It is also significant that, with the first brominating step, the HBr eliminated may protonate the coordinated ligand away from Ni, and this is the origin of Br^- at Ni and also of the protonated free ligand. Finally, note that the pyridinium cation in the observed product *fails* to protonate the pyrrolide N coordinated to nickel in the complex anion. In summary, this reactivity at the pyrrolide ring of ligand is anticipated by the frontier orbital composition discussed above (Figure 3), as is the selectivity for bromination at pyrrolide vs at pyridyl. What occurs is classical electrophilic aromatic substitution at pyrrole.

Regarding this ligand loss and HBr elimination, it has been shown that,[4] upon approach of a nucleophile, a pyridylpyrrolide in planar PtL_2 can revert to monodentate binding, through only the pyrrolide nitrogen, with pendant pyridyl functionality (Scheme 3). However, when confronted by a Brønsted *acid*, the

Scheme 3

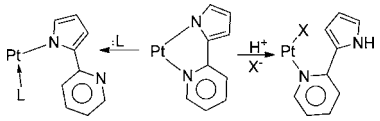

chelate can open up with only pyridyl coordinated, and the pendant pyrrolide carries the proton. This apparently facile conversion to two different monodentate binding modes distinguishes the pyridylpyrroles from bipyridyls, a valuable difference which might be exploited productively with the former. While this may be especially favored by interligand steric tension for *planar* $Pt(L)_2$ complexes, it must be kept in mind even for the nonplanar molecules reported here.

Pyridine N-oxide. $Ni(L^2)_2$ reacts in time of mixing with pyridine N-oxide give $Ni(L^2)_2(PyNO)_2$. NMR spectroscopic studies show that a 1:1 reaction in CH_2Cl_2 (or benzene) gives one product, which a second equivalent of amine oxide then converts to a distinct species. NMR spectra always show only averaged signals for the several species present, with chemical shifts moving by large amounts, because of the paramagnetism of each.

Crystals were grown by layering a CH_2Cl_2 solution with pentane. The product (Figure 9) shows the coordination of two

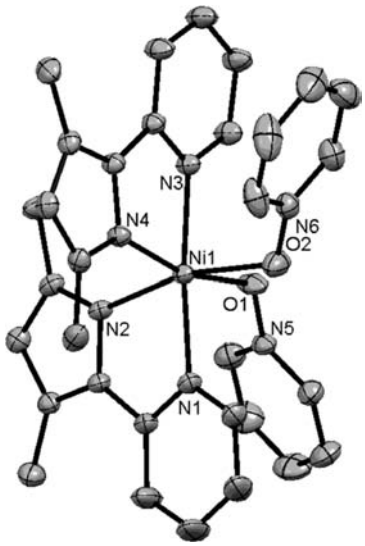

Figure 9. ORTEP view (50% probabilities) of the structure of $Ni(L^2)_2(C_5H_5NO)_2$ with hydrogens and fluorines omitted for clarity. Unlabeled atoms are carbons. Selected structural parameters: Ni1−O1, 2.1011(12) Å; Ni1−O2, 2.1334(13); Ni1−N1, 2.0660(13); Ni1−N2, 2.0816(13); Ni1−N3, 2.0797(13); Ni1−N4, 2.0727(12); O1−Ni1−O2, 87.29(6); O1−Ni1−N1, 90.24(5); O2−Ni1−N1, 87.28(5); O1−Ni1−N2, 88.86(5); O2−Ni1−N2, 165.95(5); N1−Ni1−N2, 79.22(5); O1−Ni1−N3, 85.96(5); O2−Ni1−N3, 88.59(5); N1−Ni1−N3, 174.52(5); N2−Ni1−N3, 104.61(5); O1−Ni1−N4, 165.03(5); O2−Ni1−N4, 91.28(5); N1−Ni1−N4, 104.58(5); N2−Ni1−N4, 95.85(5); N3−Ni1−N4, 79.11(5).

molecules of pyridine N-oxide to nickel, but no oxo transfer. This confirms the Lewis acidity of $Ni(L^2)_2$, but the formation of a bis-adduct actually goes beyond the 1:1 stoichiometry predicted by the 18 electron rule. The resulting six-coordinate molecule has cis amine oxide stereochemistry, apparently because of steric interference which would exist in a planar arrangement of two L^2 ligands in the trans isomeric alternative; moreover, on the energetically beneficial side, this positioning places the electron withdrawing CF_3 groups above the electron rich π system of the L^2 pyridyls. Distances from Ni to the L^2 nitrogens are similar to both pyrrolide and pyridyl nitrogens. The Ni/O distances are slightly (∼0.02−0.05 Å) longer than those to nitrogen, and the N/O distances (∼1.32 Å) are identical to those in free pyridine N-oxide (1.316 Å).[66] Angles Ni−O−N are 121−124°, and thus consistent with sp^3 hybridization at oxygen. The pyrrolides are mutually cis, but the pyridines are mutually trans. It is interesting to note that the structure of the water and THF adducts involve decreasing the angle between two pyridyls, while the pyridine N-oxide structure involves decreasing the angle between two pyrrolides; in this way the product structures differ. In the amine oxide case, this may relate to complementary trans effects of pyrrolide and amine oxide.

A sample of $Ni(L^2)_2(PyNO)_2$ was heated for 12 h in benzene at 60 °C, but showed no change (e.g., no completion of the desired oxo transfer).[67] In Figure 9, there are signs of π-stacking between each pyridine N-oxide and one pyridyl ring; the closest approach of ring atoms within a pair is 3.05 Å and 3.06 Å, and is between nitrogens. This may polarize the L^2 ligand and thus make scission of the O/N bond of the oxidant unfavorable.

dx.doi.org/10.1021/ic4011746 | Inorg. Chem. 2013, 52, 9511−9521

Other oxidants. Other oxidants studied were AgOTf (in dichloromethane) and C_2Cl_6 (in benzene) at 1:1 stoichiometry, and both show no change by NMR after 48 h. Reaction with $PhICl_2$ gave color change to a product with solubility and NMR spectra analogous to that of the Br_2 product, so apparently the result of ring chlorination. Perhaps a less aggressive halogen might redirect reactivity to the metal. Mixing of $Ni(L^2)_2$ with equimolar I_2 in benzene at 25 °C shows no reaction. If these two reagents are combined in toluene, NMR spectra at −40 °C show no change from the spectra in the absence of I_2 and thus indicates no formation of even an η^1 adduct $(L^2)_2Ni(I_2)$.[68]

DISCUSSION AND CONCLUSIONS

The transmission of spin density from metal into the ligand is evident from the large range of proton NMR chemical shifts. Fluorine chemical shifts are also perturbed significantly, but less so, because of the buffering effect of intervening σ bonds. The detection of two oxidative cyclic voltammetry events (Figure 6) is also supportive of ligand redox activity, since one cannot imagine *two* metal-centered oxidations of Ni(II). The focus of bromination, not at the metal, but rather at the pyrrolide, is also consistent with HOMO participation by the pyrrolides, and indicates that, at least for Br_2 reagent, it will be necessary to protect *all* pyrrolide ring carbons, to direct reactivity to the metal. The reluctance of pyridine N oxide to transform from coordinated ligand to complete an oxo transfer event indicates the need to examine other, more potent oxo transfer reagents. Adduct formation between pyridine N-oxide and $Ni(L^2)_2$ shows kinetic lability and that an inner sphere mechanism for oxidation is viable.

The attack of Br_2 oxidant on the ligand seen here is related to the observed analogous substitution of oxidant on *meso* carbons of metal porphyrins complexes. In general, it shows the need to "bulletproof" a ligand to hostile reactive environment needed for particular applications. A good example of this is seen in the catalyst optimization (against ligand degradation) chemistry of Collins[69] as well as the history of increasingly brominating porphyrins to make them robust for oxidation catalysis with O_2.[70,71] In the case at hand, the resulting brominated ligand would appear to have potential as offering completely protected ring carbons. Independent experiments reveal that Br_2 reacts immediately with HL^2 to form the same ring brominated compound $^{Br}L^2H$, as its HBr salt.

EXPERIMENTAL SECTION

General Procedures. All manipulations were carried out under an atmosphere of purified argon using standard Schlenk techniques or in a glovebox. Solvents were purchased from commercial sources, purified using Innovative Technology SPS-400 PureSolv solvent system or by distilling from conventional drying agents and degassed by the freeze−pump−thaw method twice prior to use. Glassware was oven-dried at 150 °C overnight. NMR spectra were recorded in C_6D_6 and CD_2Cl_2 at 25 °C on a Varian Inova-400 spectrometer (^{1}H: 400.11 MHz, ^{19}F: 376.48 MHz). Proton and carbon chemical shifts are reported in ppm versus Me_4Si, but initially referenced to solvent protic impurity; ^{19}F NMR chemical shifts are referenced relative to external CF_3CO_2H. Mass spectrometry analyses were performed in an Agilent 6130 MSD (Agilent Technologies, Santa Clara, CA) quadrupole mass spectrometer equipped with a Multimode (ESI and APCI) source. Electrochemical studies were carried out with an Autolab model PGSTAT30 potentiostat (Eco Chemie). A three-electrode configuration consisting of a working electrode (platinum button electrode), a $Ag/AgNO_3$ (0.01 M in MeCN with 0.1 M n-Bu_4NPF_6) reference electrode, and a platinum coil counter electrode was used. All electrochemical potentials were referenced with respect to the Cp_2Fe/Cp_2Fe^+ redox couple, added internally to the sample at the end of an experiment. Electron paramagnetic resonance (EPR) spectra of the $Ni(L^n)_2$ complexes, at both X- (~9 GHz) and Q-band (35 GHz) microwave frequencies were recorded, respectively, at 77 and 2 K, but gave no signals; this negative result is not surprising for $S = 1$ systems with large zero-field splitting. Chelate ligands were synthesized from published procedures;[5] we reported earlier[32] the error of the CF_3 location published for HL^1. $SOCl_2$ was distilled under argon before use, KH, AgOTf, C_2Cl_6, and CO were purchased from commercial vendors and used without further purification, $PhICl_2$ was synthesized from a published procedure.[72] PyNO was distilled in vacuum, and Br_2 was dried over H_2SO_4.

Anhydrous $NiCl_2$ as THF Adduct. A 2.5 g portion of $NiCl_2$ was refluxed in 40 mL of freshly distilled $SOCl_2$ for 12 h. The mixture was cooled and excess $SOCl_2$ was decanted, and the residue was dried in vacuum at 50 °C for 2 h. A 70 mL portion of dried THF was placed into the flask, and the mixture was heated to reflux in Ar with vigorous stirring for 48 h, during which time the mixture became a suspension. Light yellow-brown solid was filtered and dried in vacuum (0.1 mmHg) for 12 h to give $NiCl_2(THF)_{0.7}$.[73]

$Ni(L^0)_2$. (Scheme 4) A 100 mg portion of L^0H (0.39 mmol) in 10 mL of THF was slowly added to the stirring mixture of 16.4 mg of KH

Scheme 4

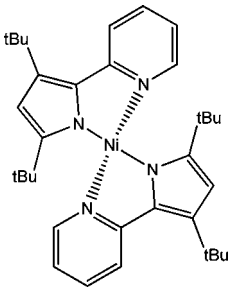

(1.05 equiv., 0.409 mmol) in 10 mL of THF. After 30 min gas evolution had ended and full conversion into L°K was observed. The solution was filtered and used without further purification (removal of solvent yields solid L°K). A 35.1 mg portion of $NiCl_2(THF)_{0.7}$ (0.195 mmol) was added to the stirring solution of L°K. The color turned from light yellow to dark green after 2 min. After 2 h of vigorous stirring all volatiles were removed in vacuum, the residue was treated with 20 mL of benzene, solid KCl was filtered off, and the resulting green solution was dried in vacuum (0.1 mmHg) for 1 h to give a green powder of $(L^0)_2Ni$. Yields, here and below, are generally quantitative, to furnish a single product. **^{1}H NMR (C_6D_6)**: 1.99 (br.s, 9 H, ^{t}Bu), 6.39 (br.s, 1 H, C−H Ar), 22.82 (br.s, 9 H, ^{t}Bu), 68.5 (br.s, 1 H, C−H Ar), 71.56 (br.s, 1 H, C−H Ar), 89.88 (br.s, 1 H, C−H Ar), 219.76 (br.s, 1 H, C−H Ar). **MS (APCI-positive ion, THF)** Exp: 568.3 $C_{34}H_{46}N_4Ni$ or $[M]^+$ Calc: 568.3076; Exp: 569.3 $C_{34}H_{47}N_4Ni$ or $[M+H]^+$ Calc: 569.3154. **^{1}H NMR of L^0K (THF d-8):** 1.23 (s, 9 H, ^{t}Bu), 1.34 (s, 9 H, ^{t}Bu), 5.83 (s, 1 H, C−H pyrrole), 6.63 (s, 1 H, C−H Ar), 7.32 (t, J = 7.4, 1 H, C−H Ar), 7.73 (d, J = 8.0, 1 H, C−H Ar), 8.23 (d, J = 4.0, 1 H, C−H Ar).

$Ni(L^1)_2$. (Scheme 5) A 100 mg portion of L^1H (0.37 mmol) in 10 mL of THF was slowly added to the stirring mixture of 15.7 mg of KH (1.05 equiv., 0.390 mmol) in 10 mL of THF. After 30 min, gas evolution had ended and full conversion into L^1K was observed. The solution was filtered and used without further purification (removal of solvent furnishes solid L^1K). A 33.6 mg portion of $NiCl_2(THF)_{0.7}$ (0.186 mmol) was added to the stirring solution of L^1K. The color turned from light yellow to dark red after 5 min. After 2 h of vigorous stirring all volatiles were removed in vacuum, the residue was treated with 20 mL of benzene, solid KCl was filtered away, and the red solution was dried in vacuum 0.1 mmHg for 1 h to give gray powder $(L^1)_2Ni$. **^{1}H NMR (C_6D_6)**: 7.07 (br.s, 1 H, C−H Ar), 23.58 (br.s, 9 H, ^{t}Bu), 66.51 (br.s, 1 H, C−H Ar), 67.90 (br.s, 1 H, C−H Ar), 91.90

dx.doi.org/10.1021/ic4011746 | Inorg. Chem. 2013, 52, 9511−9521

Scheme 5

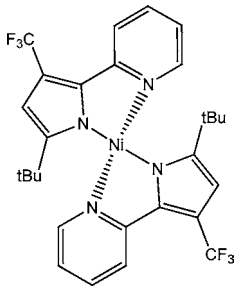

(br.s, 1 H, C−H Ar), 210.42 (br.s, 1 H, C−H Ar). **^{19}F NMR (C_6D_6):** −12.2 (s). **MS (APCI-positive ion, THF)** Exp: 592.2 $C_{28}H_{28}F_6N_4Ni$ or $[M]^+$ Calc: 592.1572; Exp: 593.2 $C_{28}H_{29}F_6N_4Ni$ or $[M+H]^+$ Calc: 593.1650. **^{1}H NMR of L^{1}K (THF d-8):** 1.27 (s, 9 H, ^{t}Bu), 6.13 (s, 1 H, C−H pyrrole), 6.81 (m, 1 H, C−H Ar), 7.47 (t, J = 7.1, 1 H, C−H Ar), 7.58 (d, J = 8.2, 1 H, C−H Ar), 8.29 (d, J = 3.3, 1 H, C−H Ar). **^{19}F NMR (THF d-8):** −51.1 (s).

Ni(L^2)$_2$(THF). (Scheme 6) A 100 mg portion of L^{2}H (0.357 mmol) in 10 mL of THF was slowly added to the stirring mixture of 15.0 mg

Scheme 6

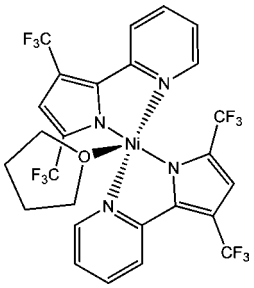

of KH (1.05 equiv., 0.374 mmol) in 10 mL of THF. After 30 min, gas evolution had ended and full conversion into L^{2}K was observed. The solution was filtered and used without further purification (vacuum here furnishes solid L^{2}K). A 32.1 mg portion of $NiCl_2(THF)_{0.7}$ (0.178 mmol) was added to the stirring solution of L^{2}K. After 12 h of vigorous stirring at 60 °C all volatiles were removed from light yellow-green solution in vacuum, the residue was treated with 20 mL of benzene, solid KCl was filtered off, and the light yellow solution was dried in vacuum (0.1 mmHg) for 1 h to give a pale green powder of $(L^2)_2$Ni(THF). The compound could be crystallized from pentane at −40 °C to give crystals suitable for crystal structure determination. **^{1}H NMR (THF d-8, 25 °C):** 11.89 (br.s, 2 H, C−H Ar), 50.81 (br.s, 2 H, C−H Ar), 55.19 (br.s, 2 H, C−H Ar), 98.33 (br.s, 2 H, C−H Ar), 159.42 (br.s, 2 H, C−H Ar). **^{19}F NMR (THF d-8, −20 °C):** −70.5 (s), −41.2 (br. s). **^{19}F NMR (THF d-8, 25 °C):** −52.6 (br. s), −42.5 (s). **^{19}F NMR (THF d-8, +50 °C):** −42.9 (s), −41.9 (br. s). This temperature dependence shows that only one ^{19}F NMR resonance is strongly paramagnetically shifted. **^{1}H NMR (C_6D_6, 25 °C):** 0.7 (br.s, 4 H, THF CH_2), 4.5 (s, 4 H, THF CH_2), 8.6 (br.s, 2 H, C−H Ar), 52.6 (br.s, 2 H, C−H Ar), 61.6 (br.s, 2 H, C−H Ar), 103.1 (br.s, 2 H, C−H Ar), 167.4 (br.s, 2 H, C−H Ar). **^{19}F NMR (C_6D_6, 25 °C):** −39.9 (br. s), −30.8 (s). **MS (APCI-negative ion, THF)** Exp: 616.0 $C_{22}H_{10}F_{12}N_4Ni$ or $[M\text{-}C_4H_8O]^-$ Calc: 616.0067; no ion was seen under typical conditions in the positive ion mode AP CI scans. **^{1}H NMR of L^{2}K (THF d-8):** 6.63 (d, J = 0.7, 1 H, C−H pyrrole), 7.06−6.94 (m, 1 H, C−H Ar), 7.64−7.57 (m, 1 H, C−H Ar), 7.70−7.64 (m, 1 H, C−H Ar), 8.42 (ddd, J = 4.8, 1.8, 1.0, 1 H, C−H Ar). **^{19}F NMR (THF d-8):** −60.1 (s), −52.7 (s).

Ni(L^2)$_2$. (Scheme 7) A 200 mg portion of $(L^2)_2$Ni(THF) (0.29 mmol) was pumped for 24 h at 70 °C. The color changed upon heating from green to orange to give 158 mg of THF-free $(L^2)_2$Ni (88%). **^{1}H NMR (CD_2Cl_2, 25 °C):** 11.0 (br.s, 2 H, C−H Ar), 61.1

Scheme 7

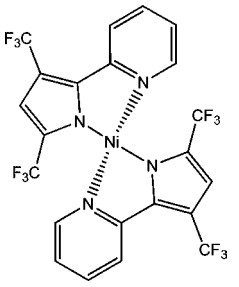

(br.s, 2 H, C−H Ar), 62.4 (br.s, 2 H, C−H Ar), 85.8 (br.s, 2 H, C−H Ar), 199.3 (br.s, 2 H, C−H Ar). **^{19}F NMR (CD_2Cl_2, 25 °C):** +45.0 (br. s), −30.5 (s). **^{1}H NMR (C_6D_6, 25 °C):** 9.7 (br.s, 2 H, C−H Ar), 59.7 (br.s, 2 H, C−H Ar), 63.2 (br.s, 2 H, C−H Ar), 90.4 (br.s, 2 H, C−H Ar), 194.4 (br.s, 2 H, C−H Ar). **^{19}F NMR (C_6D_6, 25 °C):** +45.9 (br. s), −30.9 (s). Upon addition of 8 mg of THF (~3 equiv., 0.11 mmol) to a J.Young tube containing a CD_2Cl_2 solution of 22 mg of $(L^2)_2$Ni (0.036 mmol), the color immediately turned from orange to green and NMR showed reformation of $(L^2)_2$Ni(THF). **^{1}H NMR (CD_2Cl_2, 25 °C):** 1.6 and 4.4 (br.s, 4 H each, CH_2 from THF), 9.0 (br.s, 2 H, C−H Ar), 52.8 (br.s, 2 H, C−H Ar), 79.1 (br.s, 2 H, C−H Ar), 102.8 (br.s, 2 H, C−H Ar), 166.8 (br.s, 2 H, C−H Ar). **^{19}F NMR (CD_2Cl_2, 25 °C):** −23.9 (br. s), −40.4 (s).

NMR Assay of Titration of Ni(L^2)$_2$ with THF. Spectroscopic data for $(L^2)_2$Ni as isolated after heating in vacuum, then in the presence of added 0.5, then 2.0 mols THF/Ni: **^{1}H NMR (C_6D_6):** 193/171/166 ppm; 90/102/104 ppm; 63/62/62 ppm; 59/53/52 ppm; 11/9/8 ppm. **^{19}F NMR (C_6D_6):** +5.41 and −30.0 for $(L^2)_2$Ni, −10.3 and −38.0 for 0.5 equiv of THF, and −22.4 and −39.7 for 2 equiv of THF; the fluorines thus have very different sensitivities to population changes. The ^{1}H NMR signals of free and coordinated THF are likewise averaged.

Reaction of Ni(L^2)$_2$ with Water. Twenty milligrams of $(L^2)_2$Ni (0.032 mmol) were placed into an NMR tube and dissolved in 0.5 mL of C_6D_6. A 0.6 mg portion of H_2O (0.0006 mL, 0.032 mmol) was added via syringe. The color turned from red to yellow upon shaking. NMR showed formation of a new paramagnetic species. **^{1}H NMR (C_6D_6, 25 °C):** 8.72 (br.s, 2 H), 30.84 (br.s, H_2O coord., 2 H), 52.82 (br.s, 2 H), 61.05 (br.s, 2 H), 101.85 (br.s, 2 H), 169.46 (br.s, 2 H). **^{19}F NMR (C_6D_6, 25 °C):** −39.8 (br.s), −31.8 (br.s). Assignment of the water peak was confirmed by ^{2}H NMR of the deuterated analogue on C_6H_6 using C_6D_6 for reference (^{19}F NMR is unchanged in the deuterium experiment). Addition of 2 more equivalents of H_2O changes the color to green and shows changes in the ^{1}H and ^{19}F NMR. **^{1}H NMR (C_6D_6, 25 °C):** 10.28 (br.s, 2 H), 15.39 (br.s, H_2O, 6 H), 51.20 (br.s, 2 H), 58.82 (br.s, 2 H), 99.15 (br.s, 2 H), 159.81 (br.s, 2 H). **^{19}F NMR (C_6D_6, 25 °C):** −50.8 (br.s), −42.1 (br.s). The continued change of chemical shifts for the pyridylpyrrolide protons after additional water, as well as the final color change to green, shows that the equilibrium constant for binding water is only modest.

Reaction of Ni(L^2)$_2$ with Pyridine N-oxide. Nineteen milligrams of $(L^2)_2$Ni (0.031 mmol) were placed into an NMR tube and dissolved in 0.5 mL of C_6D_6. A 2.9 mg portion of pyridine N-oxide (0.031 mmol) was added. The color turned from red to yellow upon shaking. NMR showed formation of a new paramagnetic species. **^{1}H NMR (C_6D_6, 25 °C):** −10.32 (br.s, 1 H, Py), −7.99 (br.s, 2 H, Py), 9.65 (br.s, 2 H, Py), 16.53 (br.s, 2 H), 49.62 (br.s, 2 H), 59.45 (br.s, 2 H), 103.23 (br.s, 2 H), 156.92 (v. br.s, 2 H). **^{19}F NMR (C_6D_6, 25 °C):** −39.8 and −40.8 (v. br.s). Addition of a second equivalent of pyridine N-oxide changes the color to green and shows changes in the ^{1}H and ^{19}F NMR. **^{1}H NMR (C_6D_6, 25 °C):** −20.89 (br.s, 2 H, Py), −14.45 (br.s, 4 H, Py), 12.77 (br.s, 2 H), 16.39 (br.s, 4 H, Py), 49.26 (br.s, 2 H), 51.41 (br.s, 2 H), 90.88 (br.s, 2 H), 146.47 (v. br.s, 2 H). **^{19}F NMR (C_6D_6, 25 °C):** −42.3 and −66.1 (v. br.s). Crystals of the 1:2 adduct were grown by 1:1 layering of a solution in CH_2Cl_2 with pentane.

dx.doi.org/10.1021/ic4011746 | Inorg. Chem. 2013, 52, 9511−9521

Reaction of $Ni(L^2)_2$ with Bromine. Twenty-seven milligrams of $(L^2)_2Ni$ (0.044 mmol) were placed into the Schlenk flask in 10 mL of CH_2Cl_2. A solution of known concentration of Br_2 in CH_2Cl_2 (9 mg of Br_2 or 0.044 mmol) was added to the solution dropwise at −40 °C in an atmosphere of Ar with vigorous stirring. The color of the solution turned from red to yellow, and the mixture was stirred for 30 min at −40 °C. The mixture was then allowed to warm to 25 °C and concentrated to dryness in vacuum. The residue was treated with dichloromethane (2 × 5 mL), filtered (from a small amount of precipitate), and concentrated in vacuum. NMR of the residue in CD_2Cl_2 shows the absence of starting material. Crystals suitable for X-ray diffraction analysis were grown by layering of a CD_2Cl_2 solution with pentane. **^{1}H NMR (CD_2Cl_2, 25 °C):** 8.0, 7.6, and 6.8 ppm (all v. br.) **^{19}F NMR (CD_2Cl_2, 25 °C):** −50 ppm (v. br.). Spectra in benzene were not significantly different.

Reaction of HL^2 with Bromine, Forming $[^{Br}L^2H_2]Br$. HL^2 (18.9 mg, 67.5 μmol) was placed in an NMR tube and dissolved in 0.5 mL of CD_2Cl_2 to make a colorless solution. A solution of Br_2 (11 mg, 68.8 μmol) in 0.1 mL of CD_2Cl_2 was slowly added to the HL^2 solution at room temperature. The color turned from colorless to bright yellow upon mixing to form a new product. The reaction is complete after 5 min. **^{1}H NMR (CD_2Cl_2, 25 °C):** 8.01 (m, 1 H, C−H Ar), 8.09 (d, J = 7.6, 1 H, C−H Ar), 8.52 (m, 1 H, C−H Ar), 8.81 (1 H, C−H Ar), 12.20 (br. s, 1 H, N−H pyrrole), 12.95 (v. br. s, 1 H, N−H pyridinium). **^{19}F NMR (CD_2Cl_2, 25 °C):** −55.25 (s), −59.95 (s). Addition of 1.5 mL of 10% NaOH in H_2O to remove the acidic protons yields a dark orange product. After removal of the organic layer, the final product $Na[^{Br}L^2]$ contains no acidic protons. **^{1}H NMR (C_6D_6, 25 °C):** 6.45 (dd, J = 7.6,4.4 Hz, 1 H, C−H Ar), 6.89 (td, $J_{triplet}$ = 8 Hz, $J_{doublet}$ = 2 Hz, 1 H, C−H Ar), 7.45 (d, J = 8 Hz, 1 H, C−H Ar), 8.03 (d, J = 4 Hz,1 H, C−H Ar). **^{19}F NMR (CD_2Cl_2, 25 °C):** −54.03 (s), −60.10 (s).

■ ASSOCIATED CONTENT

Ⓢ Supporting Information

Full details of computational and crystallographic studies, together with NMR spectra is provided. This material is available free of charge via the Internet at http://pubs.acs.org.

■ AUTHOR INFORMATION

Corresponding Author

*E-mail: caulton@indiana.edu. Phone: 812-855-4798. Fax: 812-855-8300.

Present Address

†Department of Chemistry, Grand Valley State University, Allendale, MI, U.S.A.

Notes

The authors declare no competing financial interest.

■ ACKNOWLEDGMENTS

This work was supported by the National Science Foundation. R.L.L. acknowledges financial support through a DOE-BES SISGR-Solar Energy Program Grant, DE-FG02-09ER16120, and Grand Valley State University Start-Up funds. The Wayne State Grid is acknowledged for computational resources.

■ REFERENCES

(1) Klappa, J. J.; Rich, A. E.; McNeill, K. *Org. Lett.* **2002**, *4*, 435−437.
(2) Luedtke, A. T.; Goldberg, K. I. *Inorg. Chem.* **2007**, *46*, 8496−8498.
(3) Schouteeten, S.; Allen, O. R.; Haley, A. D.; Ong, G. L.; Jones, G. D.; Vicic, D. A. *J. Organomet. Chem.* **2006**, *691*, 4975−4981.
(4) Chen, J.-L.; Lin, C.-H.; Chen, J.-H.; Chi, Y.; Chiu, Y.-C.; Chou, P.-T.; Lai, C.-H.; Lee, G.-H.; Carty, A. J. *Inorg. Chem.* **2008**, *47*, 5154−5161.
(5) Klappa, J. J.; Geers, S. A.; Schmidtke, S. J.; MacManus-Spencer, L. A.; McNeill, K. *Dalton Trans.* **2004**, 883−891.
(6) McBee, J. L.; Tilley, T. D. *Organometallics* **2009**, *28*, 3947−3952.
(7) Shih, P.-I.; Chien, C.-H.; Chuang, C.-Y.; Shu, C.-F.; Yang, C.-H.; Chen, J.-H.; Chi, Y. *J. Mater. Chem.* **2007**, *17*, 1692−1698.
(8) Pucci, D.; Aiello, I.; Aprea, A.; Bellusci, A.; Crispini, A.; Ghedini, M. *Chem. Commun.* **2009**, 1550−1552.
(9) Eland, J. H. D. *Int. J. Mass Spectrom. Ion Phys.* **1969**, *2*, 471−484.
(10) Von Niessen, W.; Cederbaum, L. S.; Diercksen, G. H. F. *J. Am. Chem. Soc.* **1976**, *98*, 2066−2073.
(11) Williamson, A. D.; Compton, R. N.; Eland, J. H. D. *J. Chem. Phys.* **1979**, *70*, 590−591.
(12) Cooper, C. D.; Williamson, A. D.; Miller, J. C.; Compton, R. N. *J. Chem. Phys.* **1980**, *73*, 1527−1537.
(13) Nakatsuji, H.; Kitao, O.; Yonezawa, T. *J. Chem. Phys.* **1985**, *83*, 723−734.
(14) Ford, W. K.; Duke, C. B.; Salaneck, W. R. *J. Chem. Phys.* **1982**, *77*, 5030−5039.
(15) Odom, A. L. *Dalton Trans.* **2005**, 225−233.
(16) Tang, X.; Sun, W.-H.; Gao, T.; Hou, J.; Chen, J.; Chen, W. *J. Organomet. Chem.* **2005**, *690*, 1570−1580.
(17) Perez-Puente, P.; de Jesus, E.; Flores, J. C.; Gomez-Sal, P. *J. Organomet. Chem.* **2008**, *693*, 3902−3906.
(18) Benito, J. M.; de Jesus, E.; de la Mata, F. J.; Flores, J. C.; Gomez, R.; Gomez-Sal, P. *Organometallics* **2006**, *25*, 3876−3887.
(19) Gomes, C. S. B.; Suresh, D.; Gomes, P. T.; Veiros, L. F.; Duarte, M. T.; Nunes, T. G.; Oliveira, M. C. *Dalton Trans.* **2010**, *39*, 736−748.
(20) Carabineiro, S. A.; Silva, L. C.; Gomes, P. T.; Pereira, L. C. J.; Veiros, L. F.; Pascu, S. I.; Duarte, M. T.; Namorado, S.; Henriques, R. T. *Inorg. Chem.* **2007**, *46*, 6880−6890.
(21) Carabineiro, S. A.; Bellabarba, R. M.; Gomes, P. T.; Pascu, S. I.; Veiros, L. F.; Freire, C.; Pereira, L. C. J.; Henriques, R. T.; Oliveira, M. C.; Warren, J. E. *Inorg. Chem.* **2008**, *47*, 8896−8911.
(22) Mashima, K.; Tsurugi, H. *J. Organomet. Chem.* **2005**, *690*, 4414−4423.
(23) Korobkov, I.; Vidjayacoumar, B.; Gorelsky, S. I.; Billone, P.; Gambarotta, S. *Organometallics* **2010**, *29*, 692−702.
(24) Korobkov, I.; Gambarotta, S.; Yap, G. P. A. *Organometallics* **2001**, *20*, 2552−2559.
(25) Edema, J. J. H.; Gambarotta, S.; Meetsma, A.; Van Bolhuis, F.; Spek, A. L.; Smeets, W. J. J. *Inorg. Chem.* **1990**, *29*, 2147−2153.
(26) Franceschi, F.; Guillemot, G.; Solari, E.; Floriani, C.; Re, N.; Birkedal, H.; Pattison, P. *Chem.—Eur. J.* **2001**, *7*, 1468−1478.
(27) Campazzi, E.; Solari, E.; Scopelliti, R.; Floriani, C. *Inorg. Chem.* **1999**, *38*, 6240−6245.
(28) Jiang, A. J.; Simpson, J. H.; Muller, P.; Schrock, R. R. *J. Am. Chem. Soc.* **2009**, *131*, 7770−7780.
(29) Hao, J.; Song, H.; Cui, C. *Organometallics* **2009**, *28*, 3100−3104.
(30) Jones, R. A.; Spotswood, T. M.; Cheuychit, P. *Tetrahedron* **1967**, *23*, 4469−4479.
(31) Hansch, C.; Gao, H. *Chem. Rev.* **1997**, *97*, 2995−3059.
(32) Flores, J. A.; Andino, J. G.; Tsvetkov, N. P.; Pink, M.; Wolfe, R. J.; Head, A. R.; Lichtenberger, D. L.; Massa, J. P.; Caulton, K. G. *Inorg. Chem.* **2011**, *50*, 8121−8131.
(33) King, E. R.; Betley, T. A. *Inorg. Chem.* **2009**, *48*, 2361−2363.
(34) Cohen, S. M.; Halper, S. R. *Inorg. Chim. Acta* **2002**, *341*, 12−16.
(35) Mondal, A.; Weyhermuller, T.; Wieghardt, K. *Chem. Commun.* **2009**, 6098−6100.
(36) Lu, C. C.; Weyhermuller, T.; Bill, E.; Wieghardt, K. *Inorg. Chem.* **2009**, *48*, 6055−6064.
(37) Lu, C. C.; Bill, E.; Weyhermuller, T.; Bothe, E.; Wieghardt, K. *J. Am. Chem. Soc.* **2008**, *130*, 3181−3197.
(38) Chaudhuri, P.; Wieghardt, K. *Prog. Inorg. Chem.* **2001**, *50*, 151−216.
(39) Pierpont, C. G. *Coord. Chem. Rev.* **2001**, *216−217*, 99−125.
(40) Pierpont, C. G.; Lange, C. W. *Prog. Inorg. Chem.* **1994**, *41*, 331−442.
(41) Lippert, C. A.; Soper, J. D. *Inorg. Chem.* **2010**, *49*, 3682−3684.

(42) Lippert, C. A.; Arnstein, S. A.; Sherrill, C. D.; Soper, J. D. *J. Am. Chem. Soc.* **2010**, *132*, 3879−3892.
(43) Blackmore, K. J.; Sly, M. B.; Haneline, M. R.; Ziller, J. W.; Heyduk, A. F. *Inorg. Chem.* **2008**, *47*, 10522−10532.
(44) Ketterer, N. A.; Fan, H.; Blackmore, K. J.; Yang, X.; Ziller, J. W.; Baik, M.-H.; Heyduk, A. F. *J. Am. Chem. Soc.* **2008**, *130*, 4364−4374.
(45) Haneline, M. R.; Heyduk, A. F. *J. Am. Chem. Soc.* **2006**, *128*, 8410−8411.
(46) Mukherjee, C.; Weyhermueller, T.; Bothe, E.; Chaudhuri, P. *Inorg. Chem.* **2008**, *47*, 2740−2746.
(47) Fedushkin, I. L.; Maslova, O. V.; Hummert, M.; Schumann, H. *Inorg. Chem.* **2010**, *49*, 2901−2910.
(48) Fedushkin, I. L.; Makarov, V. M.; Sokolov, V. G.; Fukin, G. K. *Dalton Trans.* **2009**, 8047−8053.
(49) Fedushkin, I. L.; Skatova, A. A.; Lukoyanov, A. N.; Khvoinova, N. M.; Piskunov, A. V.; Nikipelov, A. S.; Fukin, G. K.; Lysenko, K. A.; Irran, E.; Schumann, H. *Dalton Trans.* **2009**, 4689−4694.
(50) Stanciu, C.; Jones, M. E.; Fanwick, P. E.; Abu-Omar, M. M. *J. Am. Chem. Soc.* **2007**, *129*, 12400−12401.
(51) Sazama, G. T.; Betley, T. A. *Inorg. Chem.* **2010**, *49*, 2512−2524.
(52) King, E. R.; Betley, T. A. *J. Am. Chem. Soc.* **2009**, *131*, 14374−14380.
(53) Andrieux, C. P.; Hapiot, P.; Audebert, P.; Guyard, L.; An, M. N. D.; Groenendaal, L.; Meijer, E. W. *Chem. Mater.* **1997**, *9*, 723−729.
(54) Guyard, L.; Hapiot, P.; Neta, P. *J. Phys. Chem. B* **1997**, *101*, 5698−5706.
(55) Franklin, J. L. *J. Am. Chem. Soc.* **1950**, *72*, 4278−4280.
(56) Evans, D. F. *J. Chem. Soc.* **1959**, 2003−2005.
(57) Siedle, A. R.; Newmark, R. A.; Pignolet, L. H. *Inorg. Chem.* **1983**, *22*, 2281−2286.
(58) Cirera, J.; Ruiz, E.; Alvarez, S. *Inorg. Chem.* **2008**, *47*, 2871−2889.
(59) Wang, H.; Zeng, Y.; Ma Jin, S.; Fu, H.; Yao, J.; Mikhaleva, A. I.; Trofimov, B. A. *Chem. Commun.* **2009**, 5457−5459.
(60) Amos, A. T.; Hall, G. G. *Proc. R. Soc. London A* **1961**, *263*, 483−493.
(61) Loewdin, P.-O. *J. Appl. Phys. Suppl.* **1962**, *33*, 251−281.
(62) Martin, R. L.; Davidson, E. R. *Phys. Rev. A* **1977**, *16*, 1341−1346.
(63) Neese, F. *J. Phys. Chem. Solids* **2004**, *65*, 781−785.
(64) We present here data for the quartet species. Our calculations also identified an isoenergetic (*E*(SCF) only) doublet species where the ligand-based radical orbital is aligned antiparallel to the spins on Ni. A corresponding orbital analysis shows the overlap (an indicator of the strength of the AF coupling) to be nearly zero, and the magnetic state of this species is the target of ongoing investigations.
(65) The modest size of these changes is related to the fact that one electron oxidation is distributed over two L^2 ligands, although the delocalized radical may be the result of self-interaction errors in DFT (*Science*, **2008**, *321*, 792−794).
(66) Clegg, W.; Sheldrick, G. M.; Klingebiel, U.; Bentmann, D.; Henkel, G.; Krebs, B. *Acta Crystallogr., Sect. C: Cryst. Struct. Commun.* **1984**, *C40*, 819−820.
(67) Hong, S.; Gupta, A. K.; Tolman, W. B. *Inorg. Chem.* **2009**, *48*, 6323−6325.
(68) Gossage, R. A.; Ryabov, A. D.; Spek, A. L.; Stufkens, D. J.; van Beek, J. A. M.; van Eldik, R.; van Koten, G. *J. Am. Chem. Soc.* **1999**, *121*, 2488−2497.
(69) Collins, T. J. *Acc. Chem. Res.* **1994**, *27*, 279−285.
(70) Woller, E. K.; DiMagno, S. G. *J. Org. Chem.* **1997**, *62*, 1588−1593.
(71) Ellis, P. E., Jr.; Lyons, J. E. *Coord. Chem. Rev.* **1990**, *105*, 181−193.
(72) Zhao, X.-F.; Zhang, C. *Synthesis* **2007**, 551−557.
(73) Eckert, N. A.; Bones, E. M.; Lachicotte, R. J.; Holland, P. L. *Inorg. Chem.* **2003**, *42*, 1720−1725.

dx.doi.org/10.1021/ic4011746 | *Inorg. Chem.* 2013, 52, 9511−9521